applied sciences

Article

Optical Autocorrelation Measurement for Ultrafast Pulses at NIR Wavelengths Using GaP, GaAsP, and Si Photoconductive Detectors

Hyung-Sik Kim and Yong-Sik Lim *

Department of Mechatronics Engineering, School of ICT Convergence Engineering, College of Science and Technology, Konkuk University, Chungju-si 27478, Republic of Korea; hskim98@kku.ac.kr
* Correspondence: yslim@kku.ac.kr

Abstract: In this article, we report on an optical real-time autocorrelator readout with a 5 Hz refresh rate, equipped with a transimpedance amplified photodetector based on the two-photon absorption (TPA) of semiconductor photodiodes (PDs) for ultrashort (1 < ps) pulse measurement. By replacing the GaP PD of a commercial TPA detector with GaAsP and Si PD elements, we demonstrated that the spectral response based on the TPA of each photodetector followed the linear response of the corresponding semiconductor PD within accessible wavelength regions. The TPA spectral response of the GaAsP detector exhibited a peak at 1200 nm and a long wavelength limit near 1300 nm. The TPA spectral response of the Si detector exhibited a short wavelength limit near 1170 nm and a linear response up to 1300 nm. The two types of PD were compared with the characteristics of the GaP photodiode. These photoconductive detectors are efficient, compact, and robust sensors and can be used to diagnose the pulse characteristics of ultrafast fiber lasers and light sources near IR wavelengths.

Keywords: real-time autocorrelator; two-photon absorption; photoconductive detector; GaP; Si; GaAsP; photodiode

check for updates

Citation: Kim, H.-S.; Lim, Y.-S. Optical Autocorrelation Measurement for Ultrafast Pulses at NIR Wavelengths Using GaP, GaAsP, and Si Photoconductive Detectors. *Appl. Sci.* **2023**, *13*, 6957. https://doi.org/10.3390/app13126957

Academic Editors: Xudong Li, Qiang Liu and Zhengxiang Shen

Received: 16 May 2023
Revised: 6 June 2023
Accepted: 7 June 2023
Published: 8 June 2023

1. Introduction

Optical autocorrelation for ultrashort pulse characterization using two-photon absorption (TPA) in commercially available semiconductor devices provides a convenient, economical, and sensitive alternative to traditional techniques using nonlinear crystals. For example, its application has been reported in the autocorrelation measurement of 6 fs pulses with energies as small as a few picojoules based on two-photon-induced photocurrents in a GaAsP photodiode (PD) [1]. Ultrashort pulse measurements typically use intensity and interferometric autocorrelation (AC and IAC), in which a Michelson interferometer divides them into two pulses using a beam splitter with a relative time step and recombines them to produce an interference pattern for the second harmonic generation (SHG) in a nonlinear crystal. The SHG beam is usually measured using a PD such as Si or a photomultiplier tube (PMT). Semiconductor sensors excited via TPA or three-photon absorption (3PA) effects have attracted much interest in eliminating the use of troublesome nonlinear crystals and bulky PMTs. Different from the fragile nonlinear crystals a few tens of hundreds of microns in thickness, semiconductor sensors are cheap, solid, and insensitive to phase-matching for TPA or 3PA. Strict phase mismatching for harmonic generation tends to invoke spectral filtering to ensure that the measured autocorrelation function is incorrect and distorted. Several groups have previously reported on the application of TPA- and 3PA-based phenomena for pulse diagnostics of ultrafast optical pulses with PDs using Si [2,3], GaAsP [1,2,4–6], GaP [7], InGaAs [8], SiC [9,10], ZnSSe [11], diamond [12], GaN [13], LEDs (light-emitting diodes) using AlGaAs [14], laser diodes composed of GaAsP [3], AlGaAs/GaAs [15], GaN [16], and photomultipliers, such as CsI, CuI, and GaAs PMTs [17,18], in standard autocorrelators. Multiple quantum-well waveguides and microcavity-structured optoelectronic devices have also been demonstrated [19,20]. Semiconductor sensors with linear absorption responses are preferred, as they offer high versatility, ease of integration with compact devices, and insensitivity to phase-matching and polarization restrictions for pulse diagnostics.

Over the last two decades, the field of pulse diagnostics has progressed rapidly, together with a multitude of ultrafast and ultrahigh laser developments. Spectrograms of frequency-resolved optical gating (FROG) [21] and spectral shearing sonograms for direct electric-field reconstruction (SPIDER) [22] have been developed to realize ultrafast oscilloscopes that display the temporal and spectral profiles of input pulses (intensity and phase) at rates of several Hertz. However, such techniques require extended setups—such as mini-spectrometers or cameras—and proprietary retrieval algorithms. These techniques still require nonlinear crystals or media to obtain spectrograms or sonograms for retrieving the amplitude and phase of ultrashort pulses. Although IAC does not provide a direct measure of the phase structure of an input pulse, it nonetheless provides useful information about coherent artifacts and the presence of coherent sub-structures, and provides a clear measure of second-order coherence characteristics for determining the pulse characteristics [23]. Stable ultrafast laser systems can be challenging to develop and maintain; this is because multiple scatter pulses with variable separations and relative phases with respect to the main pulses can be easily induced by over-pumping the power and due to the improper choice of output coupler transmittance. Moreover, modern FROG- and SPIDER-based techniques are unable to detect or retrieve unstable satellite pulses in all cases [24]. Consequently, traditional pulse autocorrelation measurements, regardless of sum-frequency wave mixing, are preferred in simple ultrafast oscilloscopes to monitor stable single-pulse trains. Recently, the TPA effect in commercial complementary metal–oxide–semiconductor (CMOS) webcams has been applied to develop a cost-effective NIR spectrometer capable of generating nonlinear spectral intensity and its modulated spectrum [25].

Most photocurrents induced by the photovoltaic TPA effect on various semiconductors are as low as sub-nano-ampere-scale, so they need to be amplified using external current amplifiers to convert the current into a voltage [26]. In the meantime, there have been few demonstrations on the developments in semiconductor detectors on the basis of photoconductive TPA phenomena, where current-to-voltage amplification occurs sequentially, and the weak current is converted to a moderate output voltage via transimpedance amplification circuits within the detector. Such semiconductor devices do not require an external current amplifier or the sensitivity of photocurrent detection electronics, depending on their photocurrent detection schemes—that is, the autocorrelator sensitivity is dependent only on the TPA sensitivity of the PDs. Shin et al. previously conducted sensitive autocorrelation measurement based on TPA using a commercial photoconductive GaP detector with a wide spectral response ranging from 600 to 1100 nm [27]. To fully resolve IAC for sub-10 fs pulses, we showed that the detector should have a bandwidth of at least ~100 kHz. Moreover, the study showed comparable output signals between the second harmonic generation using a BBO crystal and the TPA process using a GaP PD; the sensitivity between the SHG and TPA measurements differing by a factor of three.

This study entailed the development of a real-time autocorrelator equipped with gain-controllable photoconductive GaP, GaAsP, and Si detectors, where reverse-biased PDs were illuminated to induce the photocurrent excited by TPA. It delivered readouts of real-time AC and IAC traces at a refresh rate of 1–10 Hz. GaAsP and Si photodiodes were used in this study because they are suitable for pulse measurement up to 1.1 μm and 1.5 μm bands, respectively. GaP was selected as a reference photodiode for the detection of high-power pulses in the near-infrared (~800 nm) wavelength band and for the comparison of its characteristics with those of other semiconductor PDs. An internal operational amplifier circuit in a compact detector converted the photocurrent into an electric voltage (transimpedance type), controlling the amplification gain with 10 dB increments by choosing one of internal feedback resistors. While changing the PD of a commercial GaP detector to GaAsP and Si PDs, we investigated the spectral responses of those TPA-based photodetectors to determine their short or long wavelength limits and efficiency, allowing for TPA-based pulse measurement, by using a femtosecond light source tunable from 650 to 1300 nm. Based on the TPA spectral responses, we determined the long wavelength limits to be near 970 and 1300 nm for the GaP and GaAsP detectors, respectively, while the short wavelength limit was found to be near 1170 nm for the Si detector. We found that the spectral response based on TPA-based detectors followed the linear response curve of the corresponding semiconductor PD. These photoconductive detectors are simple and robust sensors with a high signal-to-noise ratio (SNR) and are highly competitive in diagnosing the pulse characteristics of ultrafast fiber lasers and light sources near IR wavelengths.

2. Materials and Methods

We adopted a GaP photoconductive amplifier (PDA25K, Thorlabs, Newton, NJ, USA) as a photoconductive detector, to implement a solid and an autocorrelator for the readout of a real-time autocorrelation stamp without an additional amplifier. The GaAsP and Si photoconductive detectors were prepared by replacing the GaP PD with GaAsP (G1115, Hamamatsu, Japan) and Si (PDA100, Thorlabs, Newton, NJ, USA) PDs. This photodetector features a low-offset output, low noise, and an adjustable transimpedance amplifier to control the gain up to 70 dB. The light source was a commercial tunable laser, InSight X3 (Spectra-Physics, Milpitas, CA, USA), which could provide pulses with durations of less than 120 fs at an 80 MHz repetition rate and a broad tuning range of 680–1300 nm.

Figure 1 shows the actual setup configuration for autocorrelation (12×16 inch^2). It follows a Michelson interferometer, as in conventional ACs equipped with a photoconductive detector. The pulse from the laser system was separated into two pulses by a 50:50 beam splitter (BS) with low group delay dispersion (GDD). They traveled to gold mirrors M1 and M2. The pulses reflected from M1 and M2 were noncollinearly overlapped and tightly focused on the surface of the detector using an off-axis parabolic silver mirror. A woofer was installed at the end of the reflection arm to undergo a delay scan and was operated by a 5 Hz sinusoidal wave from a home-built 30-watt power amplifier driven by the analog output terminal signal of the data acquisition card (NI USB DAQ 6356, 1.25 MS/s).

To obtain an accurate time step, we used a linear encoder (MS 15 TTL, RSF Electronik, Austria) with a resolution of 0.1 μm (0.67 fs < 1 fs) next to the fast-moving slider with retro-reflecting mirror M1. To evaluate the power dependence of the detector's photoconductivity, the laser light from the laser system was adjusted using a neutral density (ND) filter at the initial location of the autocorrelator. To confirm the wavelength dependence of TPA, wavelengths from 680 nm to 1300 nm were measured at intervals of 5 nm with the same laser power. By adjusting the variable beam attenuator, whose position was fixed in front of the incident autocorrelator, the intensity of the excitation light incident on the three semiconductor PDs was set to the same conditions. In the autocorrelator shown in Figure 1, since the TPA-based semiconductor PD was replaceable, three types were changed in turn, and then, mounted again. Since the distance of the replaced PD was changed, the distance of the parabolic mirror was finely adjusted so that the peak voltage signal of the pulse was maximized. Through this, the distance between the photodetector and the parabolic mirror was kept constant. During each tuning at 5 nm intervals, there was no change in the alignment of the autocorrelator and the incident excitation light. The output voltage from the detector was acquired and collected using a home-built LabVIEW application, in which the pulse width from each AC trace was fitted by assuming a Gaussian or sech-pulse shape. Most gain switching for the photoconductive detectors was maintained at a 30 dB setting to secure an adequately fast bandwidth; a transimpedance gain of 2.38×104 V/A was achieved at a low output impedance load (50 Ω) [28].

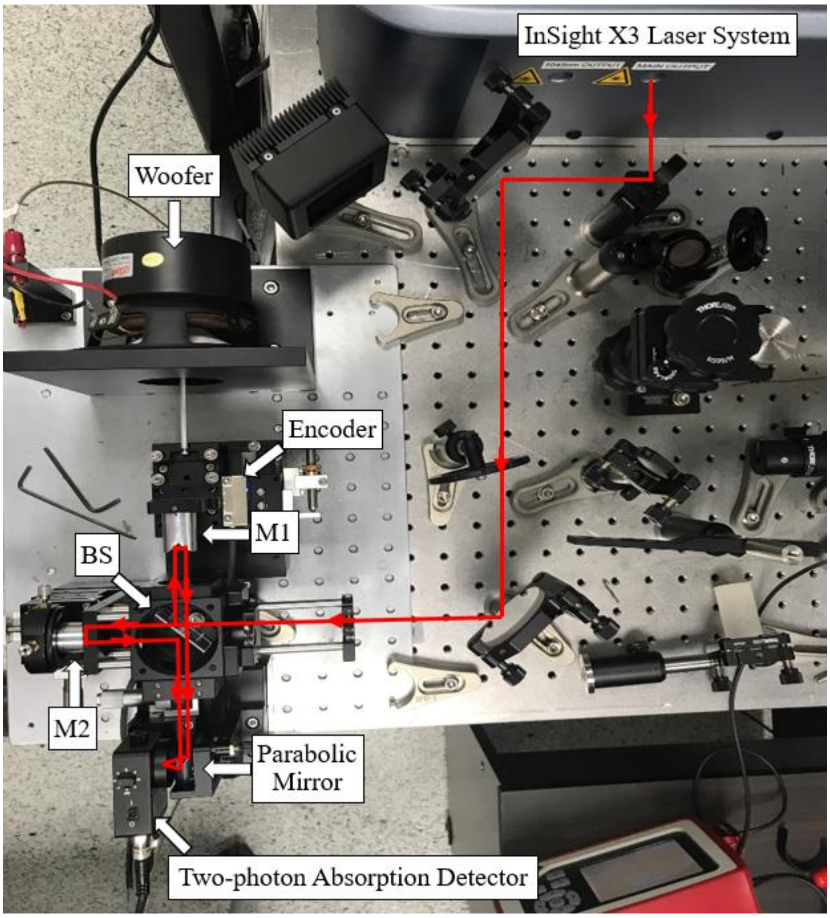

Figure 1. Real-time readout autocorrelator with a photoconductive detector to obtain TPA signals. M1 and M2 are retro-reflecting gold mirrors with a 50:50 beam splitter (BS). The focal length of the parabolic mirror and the off-axis silver mirror is 25 mm. For delay scans, a woofer is used between two separated pulses. A linear encoder is used for accurate time-step movement of the retroreflector.

3. Results and Discussion

Figure 2 shows the sequential process of extracting pulse characteristics from the readout of an AC trace based on TPA, measured using a GaAsP detector at a transimpedance gain of 30 dB, for hundreds of femtosecond pulses, with a moderate power of 300 mW, from an Insight X3 oscillator. Figure 2a shows a real-time readout of an AC trace at a 5 Hz rate across the entire ±10 ps time delay. Figure 2b shows a fitted pulse width of 430 fs, and the amplitude of the time-delay-corrected autocorrelation trace is assumed to have a Gaussian shape from the AC trace based on TPA, measured using femtosecond pulses at an 800 nm center wavelength for GaAsP PDs. Inside the femtosecond laser (Insight X3), there was an extra-cavity GDD setup outside the oscillator to control the pulse width and deliver the shortest pulses at a particular center wavelength, to meet the demands of specific applications. The AC function for a coherent light source yields a peak-to-background ratio of 2:0, while the ratio can be increased to 8:1 for the IAC function [23,29]. Most semiconductor PDs have intrinsic sharp bandgaps; however, owing to their material inhomogeneity, their linear absorption bands exhibit smooth response curves over a limited wavelength range across their inherent bandgaps—such as the spectral response curves over the 300–680 nm range of GaAsP PDs. The introduction of impurities into compound semiconductors results in the creation of additional energy levels within the material's band structure. These impurity levels, depending on the type of dopant (III or V), are commonly found in close proximity to the valence or conduction band edge [30].

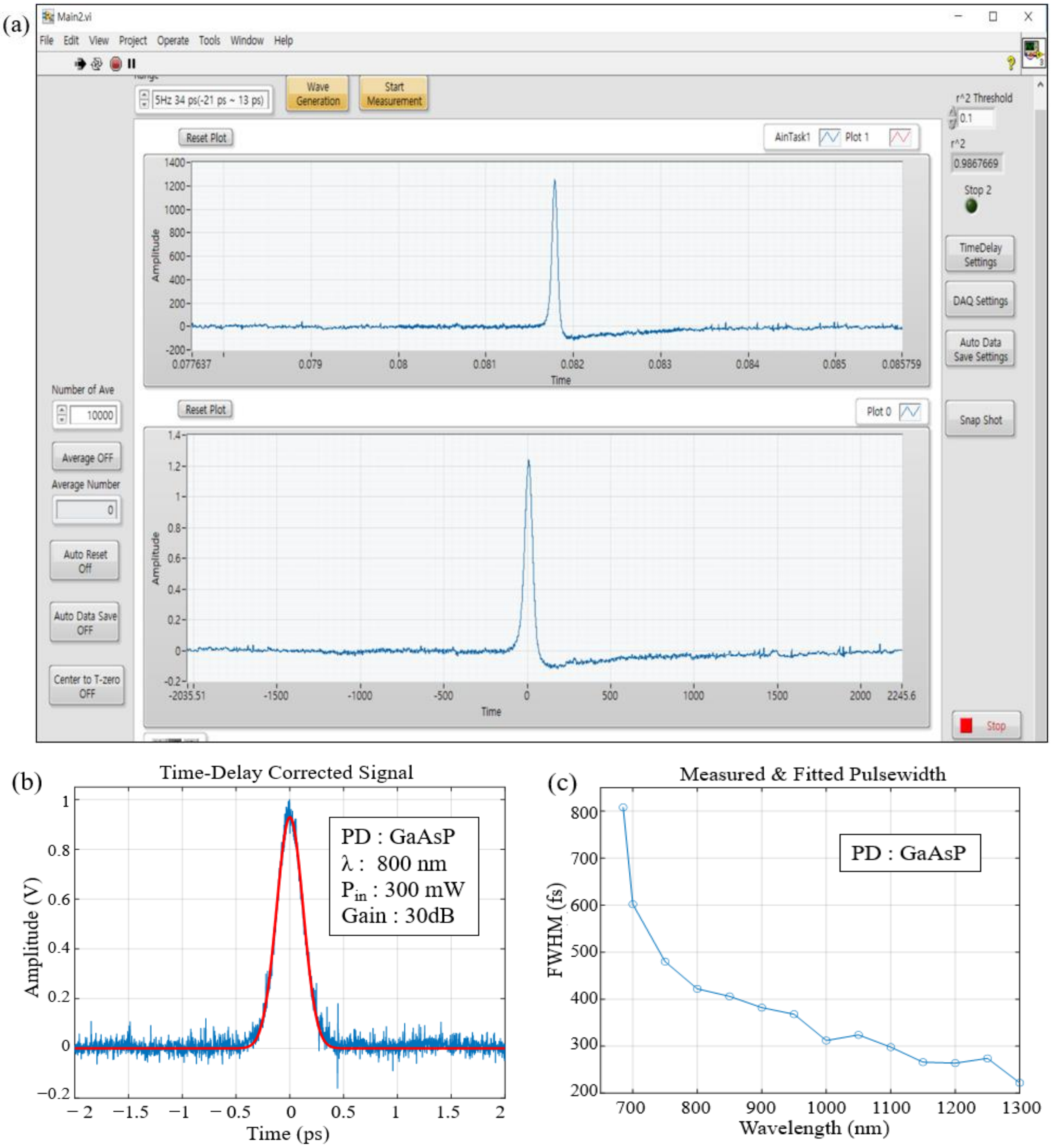

Figure 2. Subsequent processes of extracting pulse characteristics: (**a**) Readout of the AC trace at a 5 Hz refresh rate collected using a home-built LabVIEW application. (**b**) AC traces collected and fitted to the intensity AC function using Gaussian-assumed pulses, and the pulse width and amplitude of the intensity AC function. Here, the amplitude of the AC function is corrected by the squared ratio of the fitted pulse width at 800 nm to the shortest pulse width at 1300 nm, as shown in (**c**). (**c**) Variation in the pulse width with center wavelength tuning of the femtosecond laser from 680 to 1300 nm in steps of 50 nm.

However, the impurities of semiconductor PDs extend the linear response of the PD detector and exhibit considerable linear absorption, enhancing the background DC voltage of AC traces for long wavelengths above the bound of the linear response of a PD—for example, 680 nm for a GaAsP PD. These direct absorptions outside the linear PD response are detrimental and a primary challenge for two-photon measurements using semiconductor PDs.

As direct absorption due to impurity levels is rare and relatively weak at wavelengths far outside the linear response—to eliminate these unwanted linear contributions for various PDs—we normalized and fitted each AC trace such that the background DC signal strength was zero. Figure 2c shows the measured and fitted full-width-half-maximum of pulse width from the AC traces for input pulses from the Insight X3 cavity, tuned at center wavelengths of 680 to 1300 nm in steps of 50 nm. The measured and fitted pulse widths vary from ~800 to ~220 fs as the center wavelength increases, indicating that the extra-cavity GDD setup outside the oscillator is unbalanced for proper GDD compensation, and the output pulses are all severely chirped and partially GDD-compensated at the longest wavelength near 1300 nm. Accompanied by changes in the pulse width based on changes in the center wavelength for the input beam, the peak power of a femtosecond pulse is inversely proportional to the pulse width and the strength of TPA, proportional to the square of the peak power, and inversely proportional to the square of the pulse width. The sensitivity of TPA ($S_{two\text{-}photon}$)—defined as the number of generated photoelectrons per incident photon—can be calculated as follows:

$$S_{two-photon}(A/W^2) = \frac{V_{out}(V)}{P_{input}{}^2(W^2) \times Transimpedance\ Gain(V/A)}, \quad (1)$$

where P_{input} denotes the input power for TPA with repetition rate, pulse width, and beam waist, and V_{out} denotes the output voltage from the detector at each preset gain dB [28].

Accordingly, we simultaneously collected the intensity AC trace at a center wavelength to fit the pulse width and amplitude of the intensity AC function, with the extracted amplitude of the AC function reflecting the sensitivity of TPA at the center wavelength of the PD detector. The fitted amplitude of the AC function at the center wavelength was corrected by the squared ratio between the corresponding fitted and shortest pulse widths—that is, at the 1300 nm wavelength for the GaAsP PD detector—as the TPA signal is proportional to the square of the peak power. Moreover, the longer the center wavelength, the shorter the pulse width. As shown in Figure 2b, the corrected signal denotes the amplitude of the AC function at an 800 nm wavelength (on a voltage scale), corrected by the squared ratio of the fitted pulse width at 800 nm to that at 1300 nm.

As described in our previous study [27], we have shown that the output voltage at long wavelengths outside the linear response could be attributed to the TPA process of the GaP detector—based on the quadratic power dependence with a slope of approximately two; moreover, the threshold power at 40 dB for a complete AC trace is as low as 15 mW, where the PD detector responds to as low a pulse energy as ~40 pJ. In photoconductive detectors, the autocorrelator sensitivity depends only on the TPA efficiency (sensitivity). In our previous study, the sensitivity ($S_{two\text{-}photon}$) was estimated to be ~5.8×10^{-5} A/W^2 for a GaP PD [27]. For the GaP PD, the maximum sensitivity for the one-photon process is $S_{one\text{-}photon}$~0.1 A/W at 430 nm [28], which is three orders of magnitude larger than that of the TPA process. The maximum sensitivities for the one-photon process are $S_{one\text{-}photon}$~0.3 A/W at 600 nm for the GaAsP PD and $S_{one\text{-}photon} > 0.7$ A/W at 970 nm for the Si PD [31]. Since the photocarriers excited by the two-photon process across the bandgap result in tracking the linear response of the PD, we anticipate that the TPA signal for the Si PD will exhibit the most efficient sensitivity, with the GaAsP PD exhibiting higher TPA sensitivity than the GaP PD.

To ensure high performance and a wide tuning range, we collected the intensity AC traces at the same incident input power of 300 mW and fitted them to a Gaussian-assumed AC function for GaP, GaAsP, and Si detectors at three typical wavelengths along the full wavelength range of 680–1300 nm available from the oscillator. In Figure 3, the amplitude of the AC function at a given wavelength is corrected by the squared ratio of the fitted pulse width to the shortest pulse width for each PD detector. This corrected amplitude represents the TPA spectral sensitivity of the detector at a specific wavelength. Figure 3a shows a corrected amplitude near 1 V for the GaAsP detector held to a 30 dB gain at three wavelengths—that is, 685, 900, and 1300 nm. This is consistent with the fact that TPA can occur for wavelengths from 600 to 1360 nm, considering the linear response range of 300–680 nm. Notably, the signal strength at 1300 nm is slightly lower than the expectation based on the linear response curve. The amplifier gain bandwidth product in our detector is 25 MHz, and its bandwidth at 40 dB gain is reduced to 100 kHz [28], which is sufficient to resolve the fast-oscillating components in IAC with a rise time of <10 μs [27].

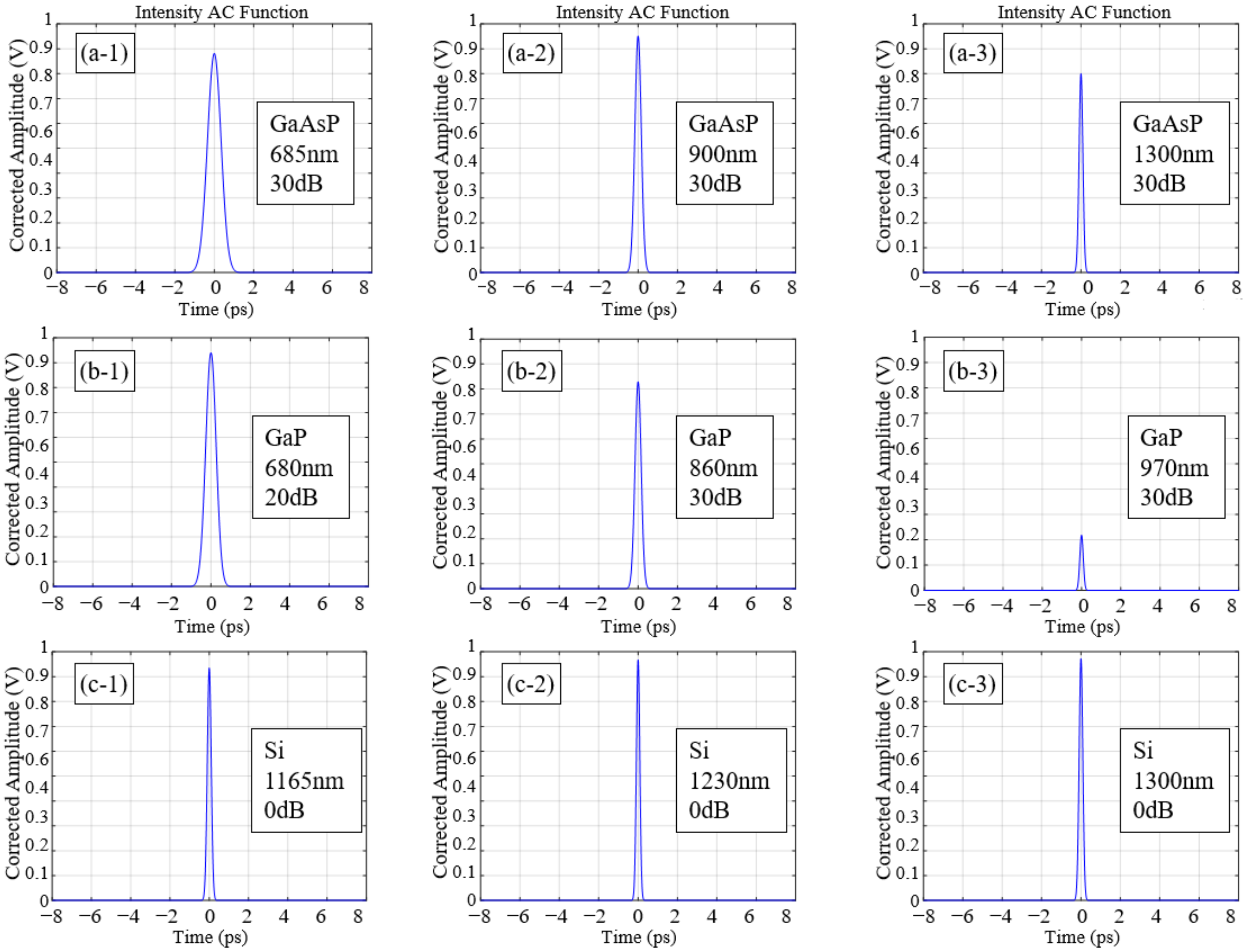

Figure 3. Corrected amplitude of the AC function, denoting the TPA signal response (**a**) for the GaAsP detector at three wavelengths—that is, 685, 900, and 1300 nm; (**b**) for the GaP detector at three wavelengths—that is, 680, 860, and 970 nm; and (**c**) for the Si detector at three wavelengths—that is, 1165, 1230, and 1300 nm. The three wavelengths are represented by serial numbers.

Figure 3b shows the corrected amplitude of the AC function for the GaP detector held to a 20–30 dB gain at three wavelengths—that is, 680, 860, and 970 nm. It is similar to that of the GaAsP detector, and its behavior can be understood within a linear response range of 150–550 nm. However, the TPA signal at 970 nm is noticeably lower than expected, with the TPA signal at 30 dB gain being too weak to enable the measurement of the pulse width at wavelengths longer than 970 nm. This is because the photodiode's responsivity varies according to the wavelength of laser light.

Figure 3c shows the corrected amplitude of the AC function, which is as high as approximately 1 V for the Si detector held to a 0 dB gain at three wavelengths—that is, 1165, 1230, and 1300 nm. Since the Si PD detector delivers the highest TPA signals, it shows sufficient strength even with a gain of 0 dB. TPA signals at shorter wavelengths than 1165 nm are too weak for measuring the pulse width because of the background DC level enhanced by strong direct absorption. The TPA signals tend to grow toward the direction of longer wavelengths, from 1165 nm to a maximum of 1300 nm. Moreover, the standard Si PD has the widest and highest linear responses among known PDs, covering a 350–1100 nm wavelength range, indicating that the TPA for Si PDs is feasible for an 1165–2200 nm wavelength range.

For a detailed investigation of the spectral response of TPA signals for photoconductive detectors, we examined the spectral dependence of the above PDs over the spectral domain, which provided the exact TPA measurements, as verified in Figure 3.

As described in Figure 3, the TPA signal in Figure 4 denotes the amplitude of the intensity AC function ($V_{peak\_corrected}$) corrected by the squared ratio of the pulse width at a particular wavelength to the shortest pulse width, fitted from the collected TPA trace for each detector. Figure 4a shows the spectral dependence of the TPA signal (sensitivity, response) over just the 730–970 nm range for the GaP detector at a 30 dB gain with a 300 kHz bandwidth. The blue circles denote the TPA signals ($V_{peak\_corrected}$) with voltage scale measured using the 20–30 nm wavelength steps. The red line represents a guideline representing a rough average value. Although the data are slightly scattered and deviated, the spectral response of TPA is similar to the linear absorption response trace of the GaP PD, as shown by the red line. The highest TPA signal of approximately 1 V at 860 nm is consistent with the peak at 430 nm of the linear response curve of the GaP PD. With the peak TPA response at 860 nm, the TPA signals moving toward longer wavelengths are rapidly reduced compared to those for shorter wavelengths. This is similar to the asymmetric linear absorption curve of the GaP PD, which exhibits a rapidly decreasing slope at the longer wavelength side lobe. It is evident that the TPA signal of the AC function on the 30 dB gain setting is reduced to be sufficiently weak to be barely distinguishable at 970 nm; however, it recovers with sufficient strength, more easily extracting the pulse width at higher gain settings than at 30 dB. Notably, a higher gain setting causes the bandwidth to reduce, with the 30/40 dB gain setting being the permissible margin to fully resolve rapidly oscillating fringes in the IAC trace [27].

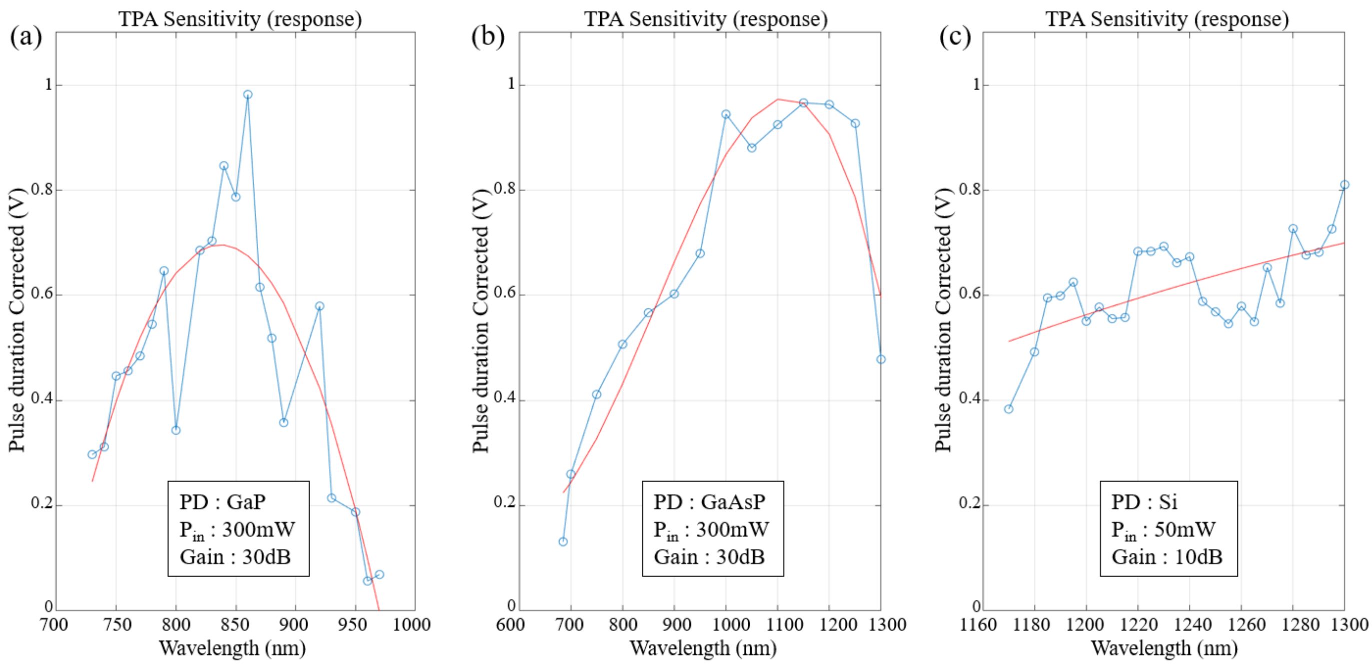

Figure 4. Spectral dependence of the TPA signal, denoting the corrected amplitude of the AC function ($V_{pulse\ duration\ corrected}$) (**a**) for the GaP detector measured in 20–30 nm wavelength steps across the 730–970 nm range, (**b**) for the GaAsP detector measured in 50 nm steps across the 685–1300 nm range, and (**c**) for the Si detector measured in 5 nm steps across the 1170–1300 nm range.

Figure 4b shows the spectral dependence of the TPA signal for the GaAsP detector measured in 50 nm steps across the 685–1300 nm range. The spectral TPA response shows smoother variations and is consistent with the movement of the linear absorption curve of the GaAsP PD, revealing an asymmetric shape similar to a right-angled triangle. The peak of the TPA signal near 1200 nm coincides with the peak of the linear response at 600 nm, showing a 10-fold TPA signal strength difference between 685 and 1200 nm. This agrees with the fact that there is a near 10-fold sensitivity difference between 340 nm (≈0.04 A/W) and 600 nm (≈0.3 A/W). Notably, the TPA response of the GaAsP PD from a visible wavelength to a 1200 nm NIR wavelength tends to increase steadily, albeit differently from the previous results of Ranka et al. [1]. Although the linear sensitivity (≈0.25 A/W) of GaAsP at 650 nm exceeds the sensitivity (≈0.18 A/W) at 475 nm, the TPA signal strength is reversed—that is, the TPA signals near longer wavelengths (e.g., 1300 nm) rapidly decrease compared to those at the peak wavelength (i.e., 1200 nm). This may be related to several shallow defect/trap levels near the band edges with a low density of states, which might be created during the PD manufacturing process [32,33]. Such imperfections/impurities in semiconductor PDs can distort and even extend to the linear response of PDs near a longer wavelength than the peak response. This is a general tendency for most semiconductor PDs.

Figure 4c shows the spectral dependence of a TPA signal for the Si detector at 10 dB gain with a 3.3 MHz bandwidth measured in 5 nm steps across a narrow 1170–1300 nm range. Since the Si PD has a linear response with high peak sensitivity (≈0.7 A/W) near 970 nm, the gain setting of the Si detector can be reduced to 10 dB, and still exhibits a TPA signal as high as a few hundred millivolts. Over the broad wavelength region from the response peak at 970 to 1060 nm and higher (≈1100 nm), the Si PD exhibits sensitivity as high as ~0.1–0.3 A/W, which is comparable to and even exceeds the peak sensitivities of GaP and GaAsP PDs. This makes the Si detector exhibit a high background-voltage rise, with the TPA signals weakening for short wavelength excitations below <1170 nm owing to strong direct absorption. The TPA signals are slightly scattered and variable because of the high TPA efficiency, with the detector position being sensitive to the shortest pulse width up to 200 fs over this wavelength region. However, a steadily increasing trend toward longer wavelengths from the red line is evident. The TPA response over a 1170–1300 nm range corresponds to the linear spectral response between wavelengths of 585 nm (≈0.25 A/W sensitivity) and 650 nm (≈0.38 A/W); however, it only shares a narrow spectral domain within an entire linear response region as narrow as 400–1100 nm. Even if the spectral region is relatively narrow, the steadily increasing TPA response resembles the corresponding steadily increasing linear spectral response.

4. Conclusions

A real-time readout autocorrelator with a 5 Hz refresh rate, based on the TPA effect, inside a commercial GaP and Si detector, as well as an alternative to a GaAsP PD, embedded with a transimpedance amplifier for switchable gain, was demonstrated. We investigated the TPA spectral responses of GaP, GaAsP, and Si photoconductive detectors by analyzing the amplitude and pulse width of an AC function, collected and fitted from TPA-induced intensity AC traces across a spectral wavelength range of 680–1300 nm. The TPA spectral response for the GaP detector exhibited a peak at 860 nm and a long wavelength limit near 970 nm, faithfully following the linear response curve across a 680–970 nm wavelength range. The TPA spectral response of the GaAsP detector exhibited a peak at 1200 nm and a long wavelength limit near 1300 nm, accurately following the linear response curve across the 685–1300 nm wavelength region. The TPA spectral response of the Si detector exhibited a peak at 1200 nm and a long wavelength limit near 1300 nm. The Si detector showed that the TPA spectral response resembled the linear response curve, based on the results obtained within the narrow 1170–1300 nm wavelength region. pulse width measurement experiment techniques using photodiodes are a long-standing research topic [1,2]. For the first time, 6 fs ultrafast pulse diagnosis was possible from a photodiode using GaAsP [1]. Subsequently, the development of an autocorrelation device for pulse width diagnosis using group 3~5 [4–7], group 2~6 [11], and group 4 compound Si semiconductor [3,9,10,12] and an MQW/a waveguide [15] was carried out consistently. These methods were performed as photovoltaic methods that detect signals without applying a reverse voltage across the photodiode. For this reason, the pulse width was measured using a sophisticatedly designed current amplifier to amplify very small currents generated from the photodiode. In this study, a transimpedance amplification method was used that effectively converts the minute current excited by the TPA phenomenon into a voltage signal by applying reverse voltage within the breakdown voltage range to both ends of the photodiode. That is, by driving in photoconductive mode, it was possible to acquire a large signal without using a separate current amplifier and an additional circuit for noise removal.

Currently, photoconductive detectors equipped with GaP and GaAsP PDs have been discontinued commercially and can be difficult to obtain, and are available online only in small quantities. However, when high-power ultrafast pulse lasers are used for only a short time, the cumulative effect caused by heat is small, so they will be used for sterilization, treatment, and diagnosis, such as processing and cutting using melting and ablation, or medical and bio-imaging fields. For this, the real-time measurement of pulses is essential. In particular, GaAsP photodetectors are remarkably compact and robust sensors that can be used to diagnose pulse characteristics for high-power ultrafast fiber lasers and measurement systems using Yb-doped solid-state lasers near 1.0–1.1 μm, while Si photodetectors are promising for use in the optical communication field using Er-doped fiber lasers and femtosecond optical parametric amplifiers near 1.5–2.0 μm.

Finally, we recognize the need to lower or eliminate the high DC offset-voltage induced by linear absorption because of PD imperfections that limit the dynamic range of autocorrelation function, as found in some of the commercial photoconductive detectors mentioned above. Moreover, new photoconductive detectors—such as GaN and AlGaN detectors for ultrashort pulse diagnoses in visible and/or ultraviolet wavelength ranges—could be developed to increase the versatility and convenience of conventional real-time autocorrelators as ultrafast oscilloscopes.

Author Contributions: H.-S.K.: Methodology; Setup Arrangement; Analysis; Validation; Writing—Review and Editing. Y.-S.L.: Conceptualization; Validation; Analysis; Writing—Original Draft, Writing—Review and Editing; Supervision. All authors have read and agreed to the published version of the manuscript.

Funding: This research received no external funding.

Institutional Review Board Statement: Not applicable.

Informed Consent Statement: Not applicable.

Data Availability Statement: The datasets generated and/or analyzed in this study are available from the corresponding author upon reasonable request.

Acknowledgments: This work was supported as a part of Konkuk University's research support program for its faculty on sabbatical leave in 2020 and by a mid-career research program grant through the National Research Foundation of Korea (NRF) funded by the Ministry of Education (MOE) (No. NRF-2021R1A2C2009136).

Conflicts of Interest: The authors declare no conflict of interest.

References

1. Ranka, J.K.; Gaeta, A.L.; Baltuska, A.B.; Pshenichnikov, M.S.; Wiersma, D.A. Autocorrelation measurement of 6-fs pulses based on the two-photon-induced photocurrent in a GaAsP photodiode. *Opt. Lett.* **1997**, *22*, 1344–1346. [CrossRef]
2. Takagi, Y.; Kobayashi, T.; Yoshihara, K. Multiple- and single-shot autocorrelator based on two-photon conductivity in semiconductors. *Opt. Lett.* **1992**, *17*, 658–660. [CrossRef]
3. Barry, L.P.; Bollond, P.G.; Dudley, J.M.; Harvey, J.D.; Leonhardt, R. Autocorrelation of ultrashort pulses at 1.5 mm based on nonlinear response of silicon photodiodes. *Electron. Lett.* **1996**, *32*, 1922–1932. [CrossRef]
4. Millard, A.C.; Fittinghoff, D.N.; Squier, J.A.; Muller, M.; Gaeta, A.L. Using GaAsP photodiodes to characterize ultrashort pulses under high numerical aperture focusing in microscopy. *J. Microsc.* **1999**, *193*, 179–181. [CrossRef]

5. Schade, W.; Preusser, J.; Osborn, D.L.; Lee, Y.Y.; deGouw, J.; Leone, S.R. Spatially resolved femtosecond time correlation measurements on a GaAsP photodiode. *Opt. Commun.* **1999**, *162*, 200–204. [CrossRef]
6. Langlois, P.; Ippen, E. Measurement of pulse asymmetry by three-photon-absorption autocorrelation in a GaAsP photodiode. *Opt. Lett.* **1999**, *24*, 1868–1870. [CrossRef] [PubMed]
7. Chong, E.Z.; Watson, T.F.; Festy, F. Autocorrelation measurement of femtosecond laser pulses based on two-photon absorption in GaP photodiode. *Appl. Phys. Lett.* **2014**, *105*, 062111. [CrossRef]
8. Reid, D.T.; McGowan, C.; Ebrahimzadeh, M.; Sibbet, W. Characterization and modeling of a noncollinearly phase-matched femtosecond optical parametric oscillator based on KTA and operating to beyond 4 /spl mu/m. *IEEE J. Quantum Electron.* **1997**, *33*, 1–9. [CrossRef]
9. Feurer, T.; Glass, A.; Sauerbrey, R. Two-photon photoconductivity in SiC photodiodes and its application to autocorrelation measurements of femtosecond optical pulses. *Appl. Phys. B* **1997**, *65*, 295–297. [CrossRef]
10. Noh, Y.C.; Lee, J.H.; Chang, J.S.; Lim, Y.S.; Park, J.D. Visible wavelength autocorrelation based on the two-photon absorption in a SiC photodiode. *J. Opt. Soc. Korea* **1999**, *3*, 27–31. [CrossRef]
11. Sun, T.; Fung, B.K.K.; Sou, I.K.; Wong, G.K.L.; Wong, K.S.; Lanzani, G. Two-photon absorption autocorrelation of visible to ultraviolet femtosecond laser pulses using ZnS-based photodetectors. *IEEE Photonics Technol. Lett.* **2002**, *14*, 86–88. [CrossRef]
12. Kleimeier, N.F.; Haarlammert, T.; Witte, H.; Schühle, U.; Hochedez, J.F.; Benmoussa, A.; Zacharias, H. Autocorrelation and phase retrieval in the UV using two-photon absorption in diamond pin photodiodes. *Opt. Exp.* **2010**, *18*, 6945–6956. [CrossRef] [PubMed]
13. Streltsov, A.M.; Moll, K.D.; Gaeta, A.L.; Kung, P.; Walker, D.; Razeghi, M. Pulse autocorrelation measurements based on two- and three-photon conductivity in a GaN photodiode. *Appl. Phys. Lett.* **1999**, *75*, 3778–3780. [CrossRef]
14. Reid, D.T.; Padgett, M.; McGowan, C.; Sleat, W.E.; Sibbett, W. Light emitting diodes as measurement devices for femtosecond laser pulses. *Opt. Lett.* **1997**, *22*, 233–235. [CrossRef] [PubMed]
15. Duchesne, D.; Razzari, L.; Halloran, L.; Morandotti, R.; Spring Thorpe, A.J.; Christodoulides, D.N.; Moss, D.J. Two-photon photodetector in a multiquantum well GaAs laser structure at 1.55 µm. *Opt. Exp.* **2009**, *17*, 5298–5310. [CrossRef]
16. Loza-Alvarez, P.; Sibbett, W.; Reid, D.T. Autocorrelation of femtosecond pulses from 415–630 nm using GaN laser diode. *Electron. Lett.* **2000**, *36*, 631–633. [CrossRef]
17. Takagi, Y. Simple autocorrelator for ultraviolet pulse-width measurements based on the nonlinear photoelectric effect. *Appl. Opt.* **1994**, *33*, 6328–6332. [CrossRef]
18. Roth, J.M.; Murphy, T.E.; Xu, C. Ultrasensitive and high-dynamic-range two-photon absorption in a GaAs photomultiplier tube. *Opt. Lett.* **2002**, *27*, 2076–2078. [CrossRef]
19. Folliot, H.; Lynch, M.; Bradley, A.L.; Dunbar, L.A.; Hegarty, J.; Donegan, J.F.; Barry, L.P.; Roberts, J.S.; Hill, G. Two-photon absorption photocurrent enhancement in bulk AlGaAs semiconductor microcavities. *Appl. Phys. Lett.* **2002**, *80*, 1328–1330. [CrossRef]
20. Krug, T.; Lynch, M.; Bradley, A.L.; Donegan, J.F.; Barry, L.P.; Folliot, H.; Roberts, J.S.; Hill, G. High-sensitivity two-photon absorption microcavity autocorrelator. *IEEE Photonics Technol. Lett.* **2004**, *16*, 1543–1545. [CrossRef]
21. Trebino, R. *Frequency-Resolved Optical Gating: The Measurement of Ultrashort Laser Pulses*; Springer: New York, NY, USA, 2000.
22. Iaconis, C.; Walmsley, I.A. Spectral phase interferometry for direct electric-field reconstruction of ultrashort optical pulses. *Opt. Lett.* **1998**, *23*, 792–794. [CrossRef]
23. Toenger, S.; Mäkitalo, R.; Ahvenjärvi, J.; Ryczkowski, R.; Närhi, M.; Dudley, J.M.; Genty, G. Interferometric autocorrelation measurement of supercontinuum based on two-photon absorption. *JOSA B* **2019**, *36*, 1320–1326. [CrossRef]
24. Escoto, E.; Jafari, R.; Steinmeyer, G.; Trebino, R. Linear chirp instability analysis for ultrafast pulse metrology. *JOSA B* **2020**, *37*, 74–81. [CrossRef]
25. Reyna-Morales, I.; Garduño-Mejía, J.; Rocha-Mendoza, I.; Rosete-Aguilar, M.; Román-Moreno, C.J.; Bravo-Hernández, A.A.; Contreras-Martínez, R.; Ordoñez-Pérez, M.; Qureshi, N. Nonlinear spectral interferometry to NIR sources. *SPIE Proc. Nonlinear Freq. Gener. Convers. Mater. Devices XXI* **2022**, *11985*, 1198508.
26. Reid, D.T.; Sibbett, W.; Dudley, J.M.; Barry, L.P.; Thomsen, B.; Harvey, J.D. Commercial semiconductor devices for two-photon absorption autocorrelation of ultrashort light pulses. *Appl. Opt.* **1998**, *37*, 8142–8144.
27. Shin, S.I.; Lim, Y.S. Simple autocorrelation measurement by using a GaP photoconductive detector. *J. Opt. Soc. Korea* **2016**, *20*, 435–440. [CrossRef]
28. Thorlabs User Guide Manual, PAD25K(-EC) GaP Switchable Gain Detector. Available online: https://www.thorlabs.com/drawings/fe177f958c8a0f70-076CF0FB-E7AB-74AC-A9D542071369CA09/PDA25K-EC-Manual.pdf (accessed on 30 May 2023).
29. Diels, J.C.M.; Fontaine, J.J.; McMichael, I.C.; Simoni, F. Control and measurement of ultrashort pulse shapes (in amplitude and phase) with femtosecond accuracy. *Appl. Opt.* **1985**, *24*, 1270–1282. [CrossRef]
30. Shur, M. *Physics of Semiconductor and Devices*; Pearson: Bengaluru, India, 2019.
31. G1115 Data Sheet for Hamamatsu Diffusion Type GaAsP Photodiodes. Available online: https://www.datasheetq.com/datasheet-download/61969/1/Hamamatsu/G1115 (accessed on 30 May 2023).

32. Casalino, M.; Coppola, G.; Iodice, M.; Rendina, I.; Sirleto, L. Near-infrared sub-bandgap all-silicon photodetectors: State of the art and perspectives. *Sensors* **2010**, *10*, 10571–10600. [CrossRef]
33. Casalino, M.; Coppola, G.; De La Rue, R.M.; Logan, D.F. State-of-the-art all-silicon sub-bandgap photodetectors at telecom and datacom wavelengths. *Laser Photonics Rev.* **2016**, *10*, 895–921. [CrossRef]